Contents lists available at ScienceDirect

International Journal of Refractory Metals and Hard

journal homepage: http://ees.elsevier.com

Cyclic contact fatigue of cemented carbides under dry and wet conditions: Correlation between microstructure, damage and electrochemical behavior

J.J. Roa [a,b,*], S. Simison [c], J. Grasso [c], M. Arcidiacono [c], L. Escalada [c], F. Soldera [d], J. Garcia [e], A.D. Sosa [c]

[a] CIEFMA-Department of Materials Science, Universitat Politècnica de Catalunya-BarcelonaTech, EEBE, Barcelona, Spain
[b] Barcelona Research Center in Multiscale Science and Engineering, Universitat Politècnica de Catalunya-BarcelonaTech, Barcelona, Spain
[c] Universidad Nacional de Mar del Plata (INTEMA-CONICET), Mar del Plata, Buenos Aires, Argentina
[d] Department Materials Science and Engineering, Saarland University, Saarbrücken, Germany
[e] AB Sandvik Coromat R&D, Lerkrogsvägen, Stockholm, Sweden

ARTICLE INFO

Keywords
Cemented carbides
Cyclic fatigue
Dry and wet conditions
Corrosion
Damage

ABSTRACT

The correlation between the damage induced under cyclic contact fatigue and their electrochemical behavior (anodic polarization curves) for different WC-Co-based cemented carbides grades was investigated at the macrometric and micrometric length scale. Under both, dry (i.e. air atmosphere) and wet (cutting lubricant fluid) conditions, the crack path propagates near the carbide/metallic binder interface, resulting in tortuous cracks of several micrometers. Despite the alkaline conditions imposed by the cutting fluid (pH 9.2), the cobalt binder is preferentially dissolved, and the carbide-skeleton keeps stable. The presence of cutting fluid in the contact fatigue zone changes the morphology of the cracks due to the partial dissolution of the binder phase. The addition of chromium to the WC-Co composition enhances corrosion resistance of the metallic binder phase resulting in reduced damage of the cemented carbides in environmental assisted cyclic contact fatigue conditions.

1. Introduction

The most used material for cutting tools is cemented carbide [1], which is a composite material with a heterogeneous structure where the carbide particles (usually WC) provide the hardness and wear resistance and the metallic binder (usually Co) contributes to the fracture toughness. The addition of alloying elements such as TiC, TaC and NbC to the WC-Co system, leads to the formation of a third phase (γ phase) that can further increase the mechanical strength of the cemented carbide composite at higher temperatures. Addition of Cr produces a refinement of the WC, but also enhances the chemical resistance and mechanical strength of the metallic binder.

The evaluation of the damage induced under cyclic contact fatigue has received increasing attention in the field of heterogeneous ceramic/metallic composite materials and in particular to WC-Co as reported in Refs. [2–5]. In this regard, a wide variety of different methods (e.g. stress-life (S—N) curves, fatigue crack growth rate as a function of cyclic stress intensity amplitude, da/dN vs. ΔK, etc.) have been used to evaluate the contact fatigue trend and in particular to quantify the number of cycles to failure for a certain cyclic stress. The most suitable methodology used along the years is the cyclic contact fatigue test, which leads to determine the crack path induced under certain stress level. This damage occurs during cyclic contact fatigue and results from the cyclic Hertzian contact stress developed when two surfaces come in contact. These fracture mechanisms may occur inclined by 45° to the contact surface where the shear stress is maximum as well as parallel and perpendicular to the contact surface as presented in Ref. [6]. One of the main difficulties in understanding contact fatigue is the large number of variables affecting cyclic contact fatigue resistance (i.e. residual stresses below surface, geometry, material properties, microstructure, inclusion sizes, operating temperature, lubricant type, lubricant additives, lubricant properties, etc.). Within this context, it is necessary to understand the damage scenario of a WC-Co composite throughout the useful life of a component that experiences cyclic contact fatigue. The modes of failure can lead to excessive noise and vibration or subsequent total failure of the mechanical system.

In cutting inserts, the cemented carbides are coated by several wear resistant layers in order to enhance their mechanical properties and keep the tool life of the insert during working conditions.

It is well known that during interrupted cutting machining (e.g. milling processes) WC-Co metals are subjected to thermo-mechanical cyclic loads, leading to the formation of cracks, mainly perpendicular to the cutting edge, known as comb cracks. In the presence of cooling

* Corresponding author at: CIEFMA-Department of Materials Science, Universitat Politècnica de Catalunya-BarcelonaTech, EEBE, Barcelona, Spain.
E-mail address: joan.josep.roa@upc.edu (J.J. Roa)

https://doi.org/10.1016/j.ijrmhm.2020.105279
Received 24 March 2020; Received in revised form 4 May 2020; Accepted 5 May 2020
Available online xxx
0263-4368/

media (also known as wet machining or cooling liquid lubrication) WC-Co materials develop additional fatigue induced cracks parallel to the cutting edge (lateral cracks) which lead to chipping and reduction of tool life of the component [7]. The formation and propagation of these damage events are accelerated by the chemical attack of the binder phase [8,9].

These systems are normally exposed to chemically aggressive media including a large variety of corrosive environments, such as lubricants, chemical and petrochemical products as well as mine- and sea-water as extensively reported in Refs. [10–13]. In this sense, in order to increase the service life and prevent the premature failure is extremely crucial to improve the corrosion resistance. During the last years, plenty of works have been published trying to understand the corrosion process under different media, since many applications of WC-Co tools involve complex service conditions, i.e. acid, caustic and neutral solutions as reported in Refs. [14–19]. However, these components usually work under cutting fluid and scarce information in this medium is available in the literature.

When considering the simultaneous action of mechanical stresses and corrosive medium, the information is scarce. Pugsley et al. [11,12] studied the effect of constant and cyclic loads on the cemented carbide in acid media and in de-ionized water and proposed that in the presence of a corrosive media the mechanical resistance is lower than in air. Gant et al. [20] also study the environmental assisted degradation of cemented carbides in tribo-corrosion conditions in solutions with different pHs (1.1, 2.6, 6.3 and 13), indicating that the degradation decreases by increasing the pH of the solution. More recently, by means of Focused Ion Beam (FIB) they revealed the subsurface cobalt dissolution in 1 M HCl solution [21].

Cemented carbides used in cutting tools for machining usually work under mechanical and thermal cycling loads in the presence of cutting fluid, indicating the need to develop tests for environmental assisted degradation in different media. To address this issue, we have expanded the conventional contact fatigue load experimental set-up, by immersing the cemented carbide/loading head in industrial cutting fluid media. The number of cycles in the test aim at corresponding to the mechanical cycling load that cemented carbides withstand during the tool life in a milling operation. Using this approach, the present work aims to investigate and understand the effect of microstructure and chemical composition on the deformation and damage resistance of selected industrial cemented carbides by applying a cyclic load under air condition and in the presence of a cutting lubricant as chemical media. The research was performed at macrometric length scale by using the cyclic fatigue test on several WC-Co cemented carbides with different chemical nature, either binder or/and ceramic carbide.

2. Experimental procedure

2.1. Specimens

WC-Co cemented carbides supplied by AB Sandvik Coromant (Stockholm, Sweden) were used in this study. Prior to the microstructural, mechanical and electrochemical investigation of the WC-Co specimens, the surface of interest was polished with silicon carbide and then with diamond suspension of 30, 6 and 3 μm. Finally, a neutral suspension of 20 nm alumina particles was used in order to remove possible work hardening introduced in the metallic binder during surface preparation.

Microstructural characterization was performed with confocal laser scanning microscope (CLSM, LEXT OL3100) and more in detail with a field emission scanning electron microscopy (FESEM). Micrographs of the WC-Co grades investigated are shown in Fig. 1. The main microstructural features were determined (i.e. binder mean free path according to empirical relations from Refs. [22,23] and the grain size for the WC phase by using the linear intercept method [24,25]). The microstructural parameters, chemical elements as well as the phases present for the cemented carbides investigated are summarized in Table 1.

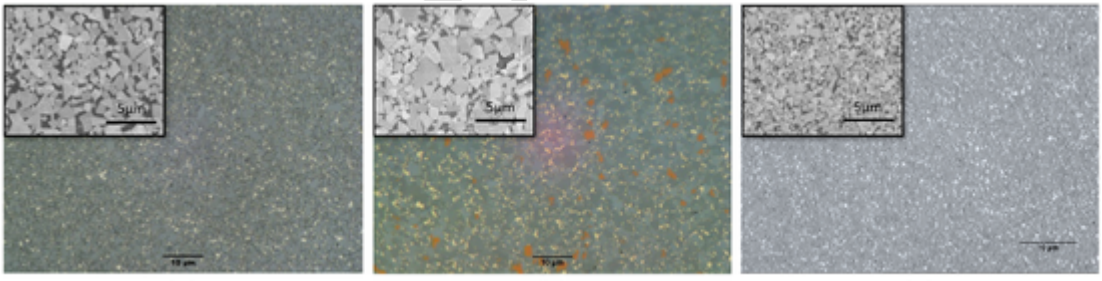

Fig. 1. CLSM and FESEM (inset) micrographs of the different WC-Co grades investigated here. (a) A, (b) B and (c) C. More information about the microstructural parameters for the different WC-Co are available in Table 1.

Table 1
Summary of the main microstructural parameters (nominal weight fraction of binder, *% wt.*; mean grain size of WC, d_{WC}; mean free path for the metallic binder and λ), chemical elements as well as the Vickers hardness in the composite materials for the different cemented carbides investigated here.

Sample	Chemical composition (wt%)					Microstructural parameters			Mechanical properties
	Co	Cr	TaC	NbC	WC	d_{WC} (μm)	λ_{Co} (μm)	Binder (vol%)	Vickers hardness, HV3
A	6.0	–	–	–	Bal.	0.74	0.25	10.5	1650
B	7.6	–	1.15	0.27		0.82	0.28	13.0	1525
C	9.0	0.9	–	–		0.44	0.18	17.5	1750

2.2. Mechanical response under contact loading

Monotonic and cyclic indentation tests at the macrometric length scale were assessed by means of spherical indentation (Hertzian tests) to identify and document damage emergence at the surface and subsurface of different WC-Co cemented carbides (e.g. circumferential cracks, cohesive spalling and/or adhesive failure). Experiments were done under contact load in both, dry and wet conditions (see Fig. 2). The cutting fluid was prepared by diluting 8 vol% stock solution in tap water (see Table 2). The pH was 9.2.

Tests were conducted in a servo hydraulic testing machine (Instron 8511) using hard metal indenters of 2.5 mm of curvature radii [26–28]. For the monotonic indentation test, the indentation force (F) gradually increased at a rate of $dF/dt \sim 30$ N/s up to the maximum indentation force ($F_{max} = 1000$ N) and gradually decreased with the same dF/dt to zero. For the cyclic indentation test, a sinusoidal wave with a 7 Hz frequency was applied to the specimen until reaching a total number of cycles (N) of 10 [5]. The force range (ΔF) was constant with an indentation force ratio of 0.2 (ΔF = *minimum force/maximum force*). Such ΔF makes the indenter remained in contact with the material surface during the entire experiment.

Numerous studies [29–32] have reported on the use of Vickers indentation to address the fracture toughness of ceramics and cemented carbides. The use of a spherical indenter -as employed in this work – presents a different fracture mechanics crack mechanism associated to the form of the indenter (no sharp corners) and the induced stress (no triaxial stress), which makes the observed crack path less comparable.

Furthermore, the experimental set-up in this work does not allow to determine crack propagation velocity in Hertzian fracture; hence the question if it is slow enough to allow for static contact fatigue effects [33–37],remains a topic for future investigations.

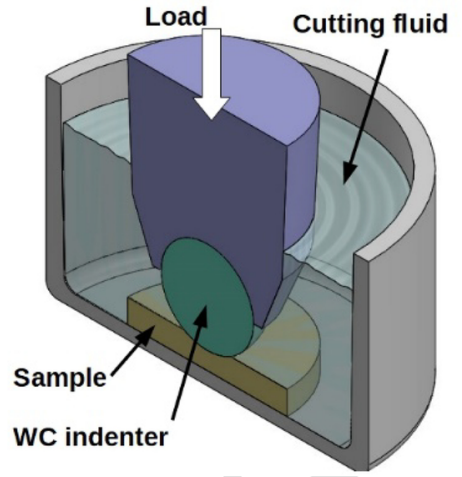

Fig. 2. Experimental set-up for the contact fatigue tests, showing the cemented carbide/loading head immersed in industrial cutting fluid media.

Table 2
Chemical composition of stock solution employed to prepare the corrosive media for the cyclic indentation tests to simulate the real working conditions.

CAS-nr.	Name	Percentage (%)
68608-26-4	Sulfonic acids, petroleum, sodium salts	< 6
122-99-6	Phenoxyethanol	< 6
6132-46-7	Fatty acids, tall-oil, compounds with triethanolamine	< 2
8012-95-1	Highly refined mineral oil	Rest.

2.3. Damage and fracture assessment

Damage evaluation related to the applied load in the monotonic and cyclic Hertz tests under dry and wet conditions was assessed by inspecting contact surfaces through CLSM.

Subsurface damage was inspected by means of focused ion beam (FIB). Cross-sectioning and microscopy were conducted using a dual beam Workstation (Zeiss Neon 40) with an ion beam current of 500 pA.

2.4. Electrochemical tests: polarization experiments

Corrosion tests were performed on the polished surface for all the different investigated specimens (Table 1). Prior to the experiments, samples were polished in order to eliminate air formed oxides and subsequently washed with ethanol. Electrochemical experiments were conducted at room temperature under atmospheric pressure in a three-electrode electrochemical cell placed inside a Faraday cage. A saturated calomel electrode (SCE) was used as the reference electrode and a platinum foil as the counter electrode. In order to avoid altering ground surface, the samples were pressed against the bottom of the cell and sealed using an O-ring. The resulting exposed area was near 28.3 mm^2. The cutting fluid was used as electrolyte. Prior the corrosion tests, the set-up was stabilized for one hour at open circuit potential (OCP). The potential was varied from OCP up to 1000 mV with a constant sweep rate of 1 $mV{\cdot}s^{-1}$.

3. Results and discussion

3.1. Polarization tests

Results of the polarization tests are summarized in Fig. 3. The samples present a broad range of corrosion potentials. Sample A is the most active, while samples B and C are +250 mV nobler. Regarding the dissolution currents, specimen C exhibited the best corrosion resistance compared to the other samples investigated here. This behavior may be related to the presence of Cr in the metallic binder which increases corrosion resistance. This observation is in fair agreement with those results reported by Sutthiruangwong et al. in 1 N sulfuric acid [38].

Fig. 4 depicts the FESEM micrographs showing the surface of samples with differences in chemical composition before (labelled as non-corroded) and after the polarization experiments (labelled as corroded).

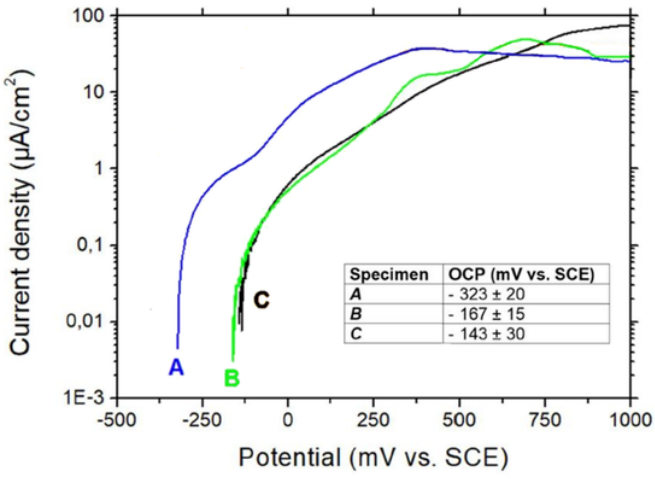

Fig. 3. Polarization curves. A to C labels in the graphs shows the different specimens investigated here. The inset summarizes the open circuit potential values "OCP" in mV vs. SCE for each specimen.

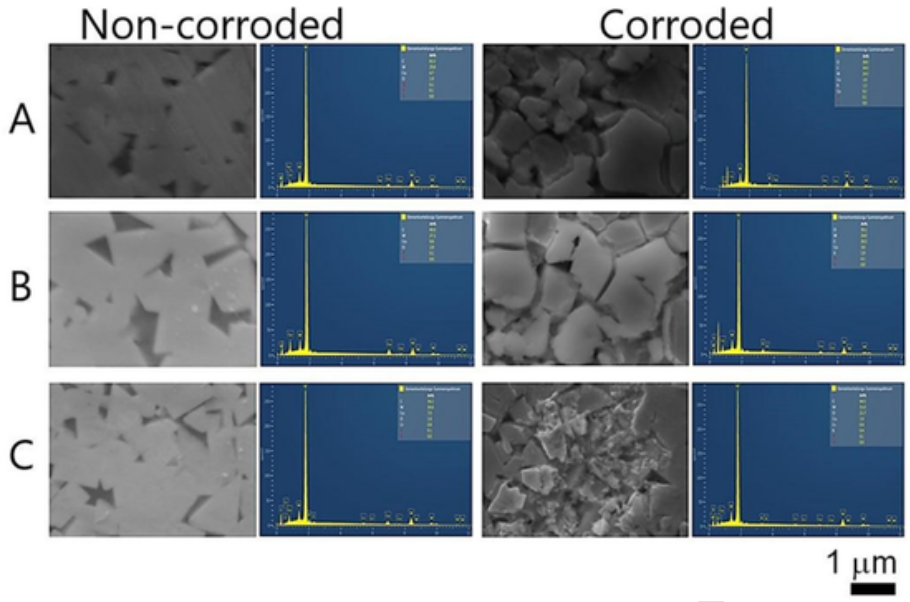

Fig. 4. SEM images and EDS spectra for non-corroded and corroded surfaces of samples A, B and C.

The FESEM micrographs for the non-corroded specimens exhibit a typical WC-Co microstructure while the corroded specimens show the effect of the cutting fluid on the metallic binder. It is clear that this fluid does not corrode the WC particles whereas the metallic binder is partially dissolved from the original microstructure. In order to get more information about the corrosion products, chemical analysis was conducted for both types of specimens. EDS spectra for each specimen are also shown on the right-hand side of each picture and a summary of their compositions (in at. %) are reported in Table 3. Data reflected a significant increase in the quantity of O that could be detected after the polarization process while the Co content also decreased demonstrating that the cobalt phase dissolved (as previously observed in FESEM micrographs) and oxides formed. It is worth noting that Cr values remained constant.

3.2. Surface and subsurface damage generated under monotonic and cyclic contact spherical indentation

The evolution of Hertzian damage at the same maximum applied load under monotonic (dry conditions) and/or cyclic contact fatigue at 1000 N performed under dry and fluid conditions was inspected by means of CLSM, showing two different trends with qualitatively similar superficial behavior as it is depicted in Fig. 5.

Post-analysis of the monotonically contact tested under dry conditions observed by CLSM displayed some interesting features depending on the content of metallic binder. The sample A with a metallic binder content of around 10.5 vol% exhibited more circumferential fissures compared to samples B and C. This phenomenon may be related to two different factors: *(i)* both samples have a higher vol. fraction of metallic binder as reported in Table 1 (13.0 and 17.5 wt%, respectively) and *(ii)* also only for specimen C the finest WC particle size compared to the other two investigated specimens. Prior to the generation of circumferential cracks the surrounding region near the spherical imprint is plastically deformed, which is in fair agreement with those observations reported by Góez and co-workers [39]. Furthermore, both specimens exhibited a hardness-toughness combined response such that (permanent) deformation induced is small and the corresponding superficial damage was absorbed through quasi-plastic mechanisms as reported in Refs. [27,39–42]. Furthermore, the damage phenomena induced during the monotonic tests is produced when the contact level generated reaches values well-above the plastic yielding onset. The tensile radial stresses and strains induce circumferential cracks in the vicinity of the residual imprints with fair agreement with the information reported in Refs [43,44]. In this sense, the specimens with higher amount of binder (B and C) are generally able to accommodate the residual deformation being a little more ductile.

Table 3
Elementary composition (at. %) determined by the EDS spectra for the non-corroded and corroded specimens.

	Non-corroded specimens			Corroded specimens		
Elements	A	B	C	A	B	C
W	29.8	27.1	30.8	24.3	24.0	31.0
Co	4.70	9.90	7.50	1.60	3.60	1.60
O	1.90	2.90	1.60	38.0	50.1	21.7
Cr	–	–	0.80	–	–	0.80

On the other hand, well developed circumferential cracks were observed in all the samples for the cyclic test under dry conditions (Fig. 5). From a direct measurement from the cross profile (right hand side Fig. 6) a pile-up at the vicinity of the imprint is quite evident. Furthermore, in the first contact cycle, the system with a low content of metallic binder and high contiguity deforms less and exhibits a greater resistance against deformation than the system with a higher volume fraction of cobalt as depicted for the investigated specimens in Fig. 6. The systems with higher volume fraction of binder (7.6 and 9 wt%) deform more as shown in the cross-profile presented for specimens B and C (3.04 and 1.74 μm, respectively). Furthermore, for the specimen C with the highest content of metallic binder, the penetration depth induced during the cyclic indentation test is smaller than that for the specimen B. Then, the low penetration depth observed for this specimen with high metallic binder content may be related to a finer WC-skeleton with enhanced deformation strength under monoaxial load (Table 1).

Specimens (A and B) cyclically tested under wet conditions present another failure mechanism at the region near the edge of the spherical imprint known as area of delamination induced by the corrosion process (detailed inspection of this zone can be clearly observed in Figs. 7 and 8, labelled as *). Similar feature was reported by Stewart et al. [45]. Specimen C shows a different behavior because the amount

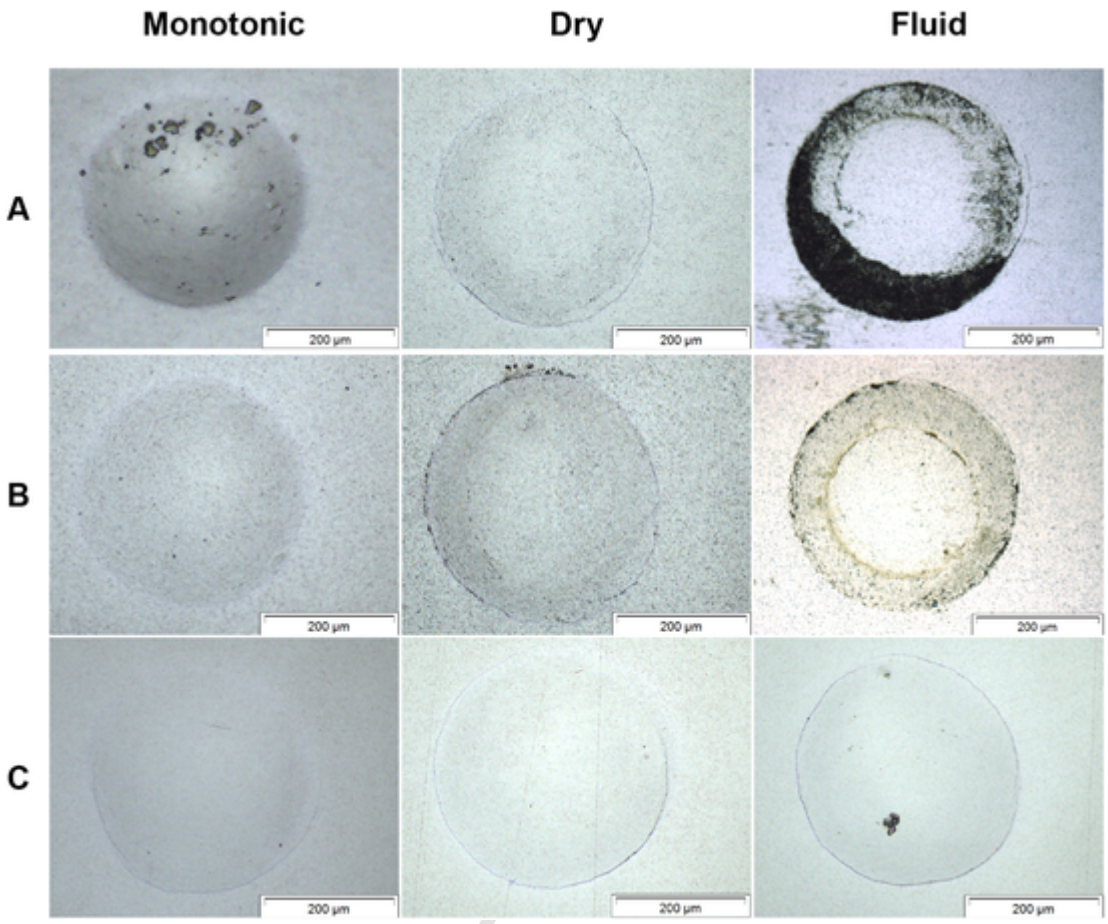

Fig. 5. Residual monotonic and cyclic contact fatigue imprints (under dry and fluid conditions) observed by CLSM microscope for the different cemented carbides investigated in this work.

of damage remains practically constant both in tests under monotonic and cyclic contact fatigue performed at the same load.

The CLSM images for specimens A and B (Fig. 5) show the two different damage mechanisms, circumferential cracks and a well delimited area of delamination of around 50 μm. This zone was examined in detail for specimen B (Fig. 7c). As it is depicted inside the area of delamination, some small features are induced during the cyclic fatigue tests, i.e. surface stress, which is identified by a high frequency of small craters as consequence of asperity contact. This damage mechanism is mainly induced due to the interaction of the spherical tip indenter and fluid against the tested material, because a wear mechanism between both bodies takes places. These evidences are in fair agreement with those reported in Ref. [45]. For specimen C no severe damage was evident and only a circumferential crack could be appreciated, highlighting the strong contribution of Cr to prevent chemical attack of the binder and hence to improve the damage under fatigue when the test is conducted under fluid.

Under dry cyclic fatigue no new cracks can be observed but the propagation is indicated by the length and the thickness of the circumferential cracks. As shown in Fig. 5 and in Fig. 7c, a completely different behavior was observed when cyclic indentation tests were carried out in contact with fluid. The common behavior is shown in detail in Fig. 8, where three different regions are visible. A non-corroded zone appears inside the spherical imprint (labelled as (1)) where the fluid induces a hydrostatic pressure between the indenter and the material being responsible of the plastic deformation. A second zone, known as a delamination area (labelled as (2)) can be seen, characterized by a loss of material in an area corresponding to a ring where the carbides are detached. As it is evident, the metallic binder suffers an anodic oxidation reaction and it is dissolved in the cutting fluid as previously reported for acid media [14,15,17]. This trend means that the effective leaching of the metallic phase takes place and thus, the onset of microcrack-like voids, in concordance with the work reported by Tarragó et al. [8]. The corroded region highlights the superficial state after cyclic contact fatigue in wet condition and the reduction of mechanical WC-Co integrity due to the interaction of the dynamic stress state and the cutting fluid against the WC-Co surface. The central part, where the indenter is permanently in mechanical contact, and the exterior of the imprint are zones free of corrosion. In the case of the central part, there is no fluid while outside the imprint (see label (3) in Fig. 8) there are no applied stresses, which is an indication of the presence of a corrosion-fatigue mechanism.

The specimen C containing high Co content as well as Cr dissolved in the metallic binder showed only circumferential cracks at the contact point, that is a low damage scenario compared to the other specimens under cycling contact load and cutting fluid. This observation can be related to two different factors: i) the presence of Cr dissolved as a solid solution in the metallic Co binder and ii) the existence of an ultrafine microstructure with a d_{WC} of near 0.44 μm as previously discussed in relation to the cross-section profiles presented in Fig. 6. Thus, the addition of alloying elements, i.e. Cr, in the metallic binder leads to an improvement of the contact fatigue resistance.

From literature, it is clear that the corrosion process of cemented carbides is dependent of the nature of the corrosive media (either acid, basic or neutral pH solutions) since the two phases are affected in different ways. Furthermore, when the cemented carbide works under

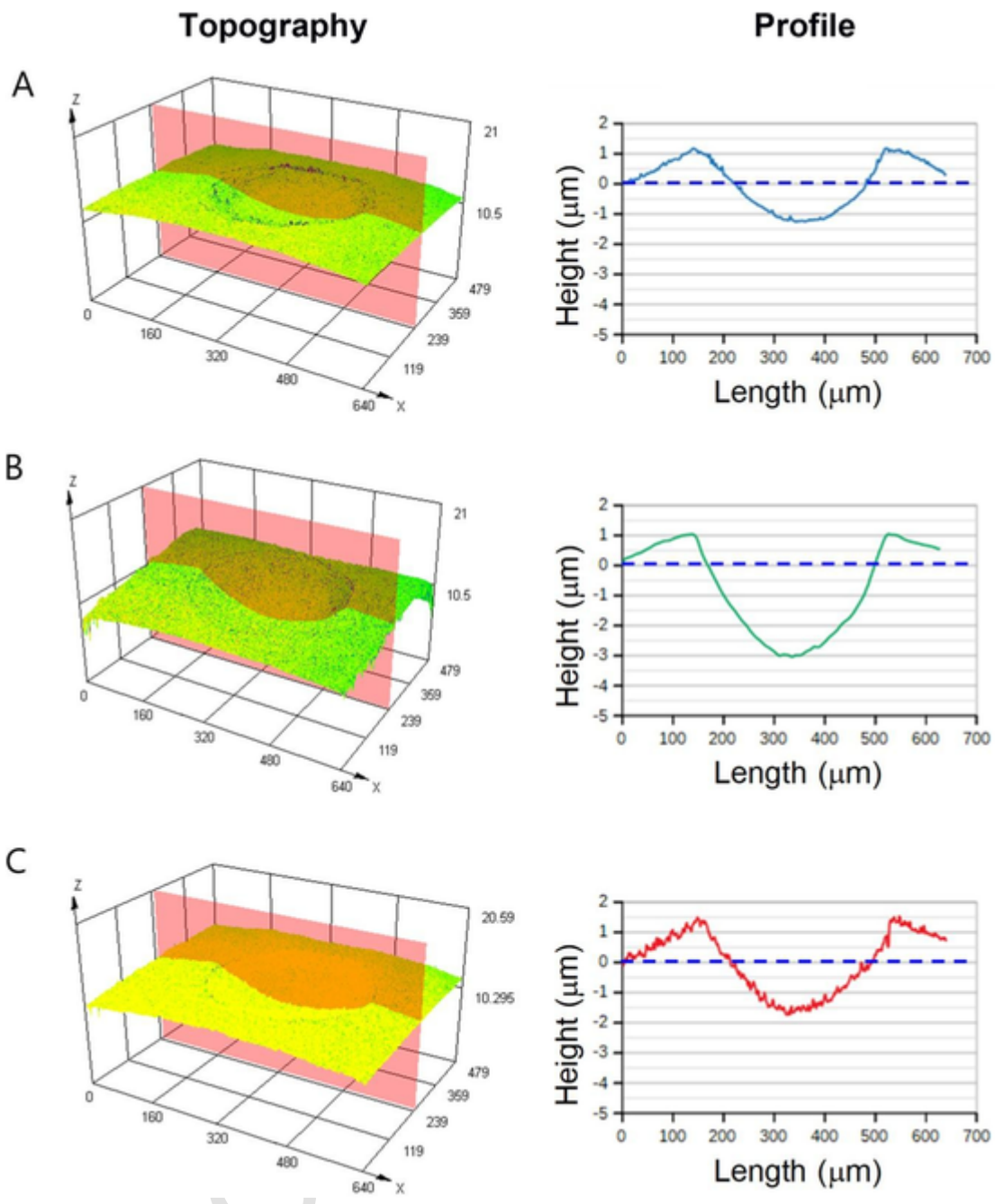

Fig. 6. Cross profile for the residual cyclic contact tests performed on several specimens under wet conditions. A, B and C.

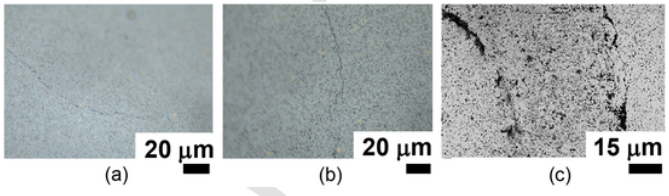

Fig. 7. Micrograph of circumferential cracks in the contact edge for the B grade observed by CLSM (a) monotonic indentation test at 1000 N, (b) Dry cyclic contact fatigue (c) cyclic contact fatigue imprint with cutting fluid.

acid condition, the corrosion phenomena is governed by a galvanic couple where the metallic binder is selectively attacked due to its anodic role, while the reinforcement ceramic particles are cathodically protected as presented in Ref. [17]. On the other hand, under basic solution, the ceramic particles dissolve while the metallic binder passivates as reported by Engqvist et al. [46] and Kellner et al. [47]. Under our experimental conditions (cyclic stress and cutting fluid of pH 9,5) it was found that the binder is the phase that is dissolved (except for sample C). The EDS-Co mapping of the affected area for sample B demonstrates that the metallic binder phase in Fig. 9 (central hand side) mainly controls the corrosion behavior of the WC-(Ta,Nb)C-Co compositions, whereas the carbides of W, Ta and Nb do not strongly react with the cutting fluid and remain chemically stable (see the right hand side map). The results of the polarization curves without applied stress show some differences among the samples that do not agree with the wet fatigue tests, except, again for sample C.

In order to understand the difference among the anodic curves of the cemented carbides (Fig. 3) and the degree of damage found in con-

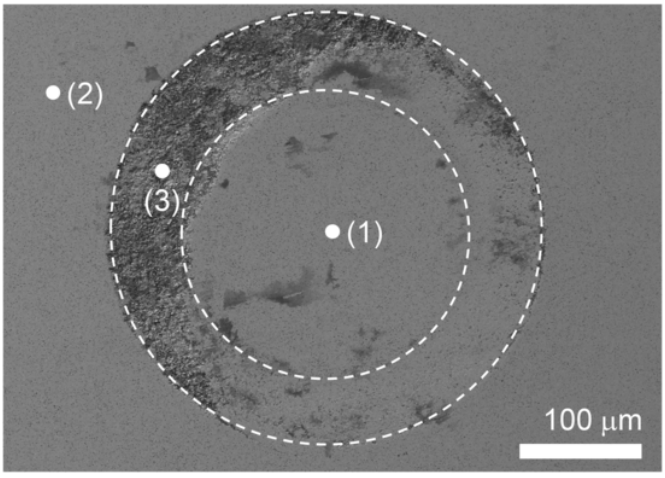

Fig. 8. Surface characterization of a non-corroded, label (1); corroded, label (2) and the non-deformed region, label (3) area for sample A (same trend has been observed for the other specimens, not shown here).

tact fatigue tests, a set of new samples was prepared. The idea was to characterize the anodic behavior of pure Co, WC and Ta(71%)Nb(22%)C in the same corrosion medium in order to determine the possible existence of a galvanic effect in real conditions. The results are depicted in Fig. 10. It can be seen that carbides are nobler than cobalt but also that the kinetics of dissolution between carbides is contrasting: (Ta, Nb)C presents a pseudopassive behavior while WC dissolves actively. Co shows a passive performance and a rupture potential at 240 mV.

From the results it can be proposed that, at the corresponding open circuit potential for the cemented carbides (Fig. 3), the binder is polarized anodically in the passive range. During contact fatigue test this passive film can be broken and reformed in every load cycle, leading to higher net dissolution of the binder and faster crack propagation. The presence of a more stable phase like (Ta, Nb)C could contribute negatively in the case of sample B.

Attempting to get a more detailed information of the referred damage scenario in the case of fatigue tests, FIB-cross sections were conducted for the different samples investigated at 1000 N in specific cracked locations, partially circumventing the residual imprints. As it is indicated in Fig. 11, it focused in the contact point where a circumferential crack was evident as presented in Fig. 5.

A detailed inspection by FESEM at low magnification (Fig. 11) showed the same damage scenario for the tests performed under dry (air atmosphere) and cutting fluid conditions. The main difference between the dry and wet conditions is the width and degree of branching of the induced cracks, which were thinner and branched for the specimens tested under wet conditions. The cyclic indentation tests showed that damage is propagated near the ceramic/metallic interface, but mainly located in the metallic binder, which is directly related to the heterogeneous microstructure present in the cemented carbides. The strain induced by cyclic indentation tests is accommodated by a combination of plastic deformation mechanisms located at the metallic binder (e.g. dislocation motion, deformation twinning, limited planar slip, etc.) [48–52], and a different fracture mechanism mainly located at the WC (e.g. carbide fracture, shearing, decohesion, etc.) in the brittle ceramic particles. These mechanisms are in concordance with those observed by Tarragó et al. [53] and Sandoval et al. [54] of WC-Co specimens plastically deformed under micropillar compression.

Examples of induced sub-superficial damage are shown at higher magnification in Fig. 12 for the different cemented carbide samples under dry and wet conditions. Close inspection of the damage induced during the contact cyclic fatigue highlights that the damage scenario for the specimens tested under cutting fluid conditions presented a higher crack density compared to the test performed under dry conditions. Furthermore, these images led to better understanding of the deformation/failure mechanisms under cyclic compression tests. Fig. 12 shows micrographs corresponding to the interior of the damage induced at the contact point. For all samples a microcrack running parallel to the carbide/binder interface (but still within the binder phase) was clearly evident. This microcrack probably stems from the propagation of the carbide/carbide interface microcrack by two mechanisms:

- binder regions near to carbide corners combined large concentrations of strains and/or stress triaxiality, indicating the presence of favorable zones for early flow and/or crack propagation as reported by Fischmeister et al. [55]
- carbide-carbide interfaces with reduced strength under compression loading, characterized as weak links in these heterogeneous ceramic/metal composite materials [34].

It is worth noting that only in the case of the more corrosion resistant binder (sample C with a Cr containing binder) the morphology of the cracks is not influenced by the cutting fluid.

4. Conclusions

In this study the influence of microstructure on environmental assisted degradation during cyclic contact fatigue for different WC-Co cemented carbides has been investigated. Contact fatigue tests were performed under dry and wet conditions by performing the tests in air and in cutting lubricant fluid, respectively. The investigation also included an electrochemical study as well as a detailed microstructure damage investigation using FIB/FESEM technique. Based on the obtained results, the following conclusions can be drawn:

(1) Contact fatigue tests show plastic and quasi-plastic deformation of the cemented carbides near the spherical imprint and the generation of circumferential cracks.
(2) Samples tested under cycling contact loads in dry conditions present well developed circumferential cracks and in the case of wet conditions also delamination in the region near the edge of the spherical imprint was observed.
(3) FE-SEM images of the plastic deformed regions show that the strain induced by cyclic indentation tests is accommodated by a combination of plastic deformation mechanisms at the metallic binder and a different fracture mechanism mainly located at the WC in the more brittle carbide particles.

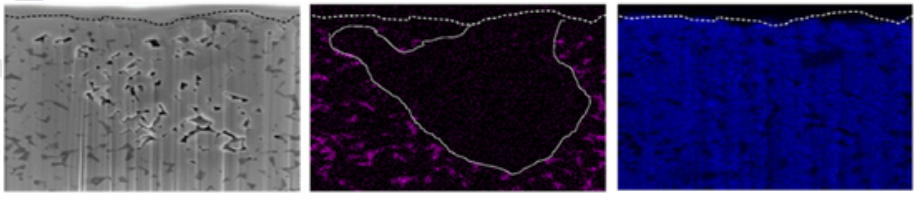

Fig. 9. Element map for Co and WC using EDS on FESEM for the cross section performed on sample B. The * denotes a region free of metallic binder.

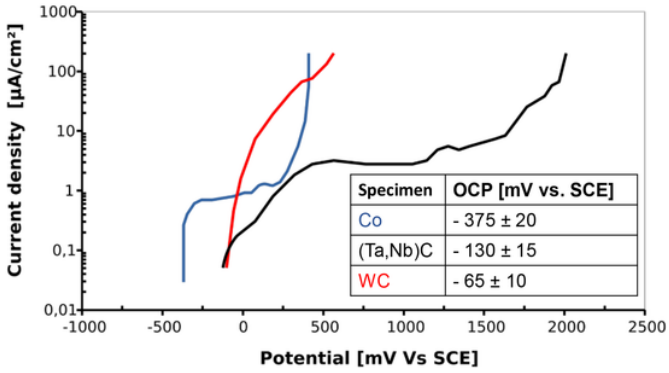

Fig. 10. Anodic polarization curves of pure Co, WC and Ta(71%)Nb(22%)C.

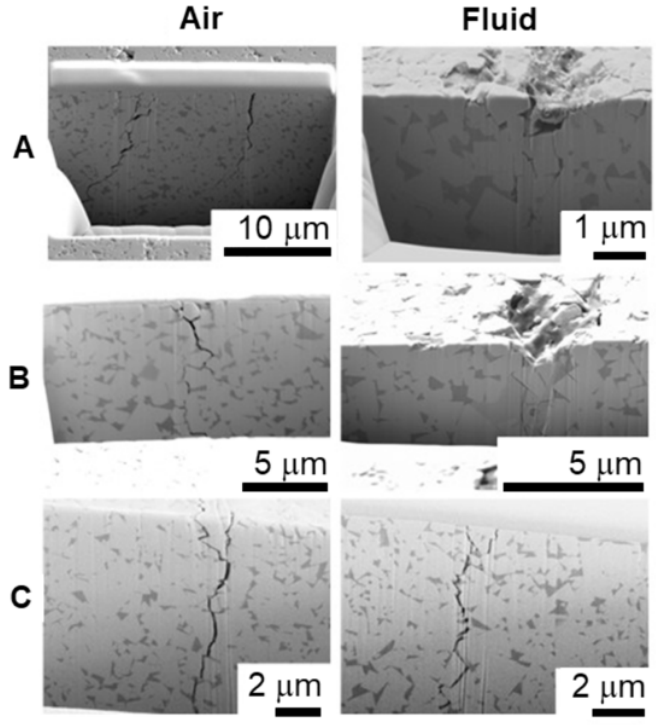

Fig. 11. Cross-section micrographs (general view) view of Hertzian contact performed at the contact edge between the indenter ball and the material under dry and cutting fluid (fluid) conditions for the different cemented carbide grades investigated here at the maximum applied load, 1000 N.

(4) The contact fatigue tests in wet conditions showed that the cutting fluid changes the morphology of the cracks, mainly due to the attack and interaction with the metallic binder.
(5) The addition of Cr to the WC-Co composition enhances the chemical-attack resistance of the metallic binder, which reduces the formation of fatigue induced cracks in the case of wet machining under contact fatigue. The beneficial effect of Cr is related to thinner and more compact oxide layers as was observed from EDS results.
(6) Despite of the alkaline conditions imposed by the cutting fluid (pH 9.2) the binder, when not alloyed with Cr, is preferentially dissolved and the carbides skeleton keeps stable.
(7) The load-free potential curves are not directly comparable with the real behavior at free potential and applied cyclic loads. Sample C containing Cr presents the best behavior in both the polarization curves as well as in the mechanical response.

Author statement

J.J.R., S.S., J.G., M.A., L.E., F.S., J.G. and A.D.S. conceived and planned the experiments. J.J.R., S.S., L.E., F.S. and A.D.S. carried out the experiments. J.J.R., S.S., J.G., M.A., L.E., F.S., J.G. and A.D.S. contributed to the analysis of the results and to the discussion section. J.J.R., S.S., J.G. and A.D.S. wrote the manuscript with input from all authors.

Declaration of Competing Interest

The authors declare that they have no known competing financial interests or personal relationships that could have appeared to influence the work reported in this paper.

Acknowledgements

This work was carried out within the framework of the CREATe-Network project (Grant number: 644013) funded by the European Commission. The current study was partially supported by the Spanish *Ministerio de Economía y Competitividad* through Grant MAT2015–70780-C4-P (MINECO/FEDER). S. Simison and D. Sosa acknowledge the University of Mar del Plata and the CONICET. M. Arcidiacono thanks the CUAA-DAHZ for exchange funding under the programme I.DEAR-Materials. J.J. Roa acknowledges the Serra Húnter programme of the Generalitat de Catalunya for the financial support.

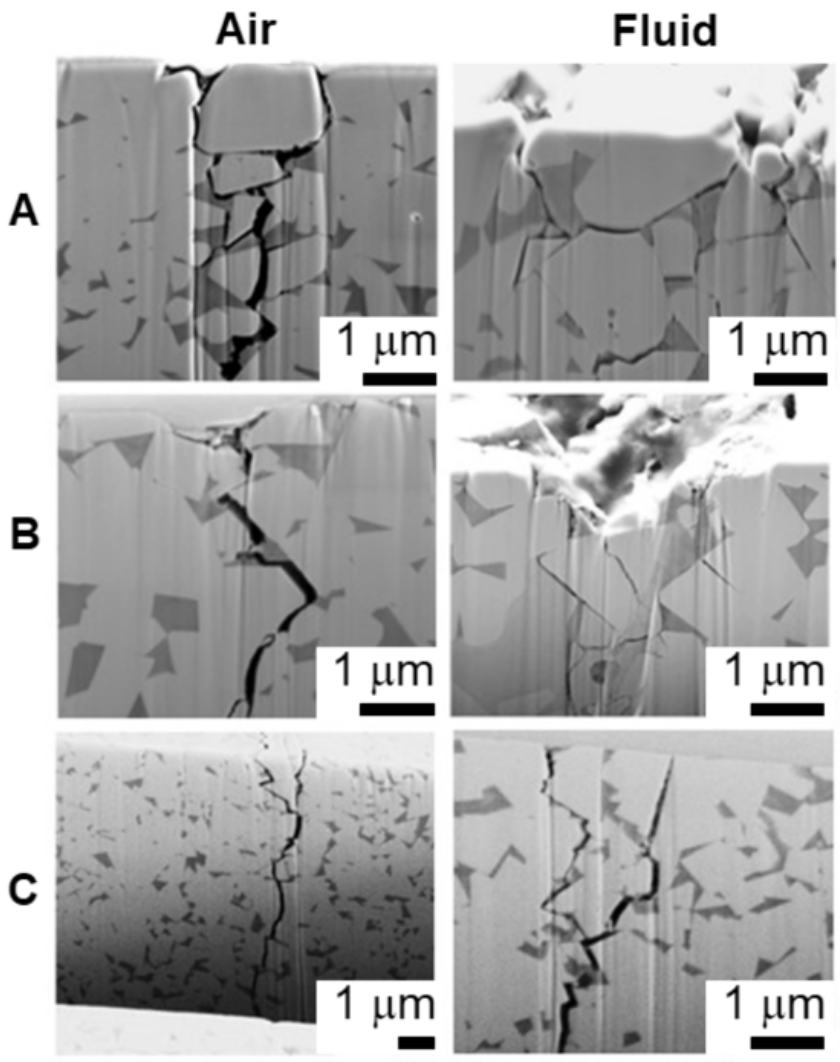

Fig. 12. Cross-section micrographs (magnification view) of Hertzian contact showing the main crack path generated during the cyclic indentation process under dry and wet (cutting fluid) conditions for the different WC-Co cemented carbides investigated here.

References

[1] J García, V Collado Ciprés, A Blomqvist, B Kaplan, Cemented carbide microstructures: a review, Int. J. Ref. Met. Hard Mater. 80 (2019) 40–68.
[2] E F Drake, A D Krawitz, Fatigue damage in a WC-nickel cemented carbide composite, Metall. Trans. A. 12A (1981) 505–513.
[3] T J Davies, S Barhana, Fatigue of a WC-25% Co alloy, Plansee Berichte Für Pulvermetallurgie. 20 (1972) 30–38.
[4] K J A Brookes, World directory and handbook of hard metals, East Barnet, Herts EN4 8BN, Int. Carb. Data, UK, 1982.
[5] I Johansson, G Persson, R Hiltscher, Determination of static and fatigue strength of hard metals, Powd. Metall. Int. 2 (1970) 119–123.
[6] Widner R. Failues of Rolling Element Bearings. Failure Analysis and Prevention, Vol. 11. ASM International.
[7] J García, C T Miranda, H Pinto, F Soldera, F Mücklich, 3D-FIB characterization of wear in WC-Co composites, Mater. Sci. Forum 825 (2015) 995–1000.
[8] J M Tarragó, G Fargas, L Isern, S Dorvlo, E Tarres, C M Müller, E Jiménez-Piqué, L Llanes, Microstructural influence on tolerance to corrosion-induced damage in hardmetals, Mater. Des. (2016) 36–43.
[9] J M Tarragó, G Fargas, E Jiménez-Piqué, A Felip, L Isern, D Coureaux, J J Roa, I Al-Dawery, J Fair, L Llanes, Corrosion damage in WC-Co cemented carbides: residual strength assessment and 3D FIB-FESEM tomography characterization, Powder Metall. 57 (2014) 324–330.
[10] U Beste, T Hartzell, H Engpvist, N Axén, Surface damage on cemented carbide rock-drill buttons, Wear 249 (2001) 324–329.
[11] V A Pugsley, G Korn, S Luyckx, H G Sockel, W Heinrich, M Wolf, H Feld, R Schulte, The influence of a corrosive wood-cutting environment on the mechanical properties of hardmetal tools, Int. J. Refract. Met. Hard Mater. 19 (2001) 311–318.
[12] V A Pugsley, H-G Sockel, Corrosion fatigue of cemented carbide cutting tool materials, Mater. Sci. Eng. A 366 (2004) 87–95.
[13] R Lu, L Minarro, Y-Y Su, R M Shemenski, Failure mechanism of cemented tungsten carbide dies in cooling liquiddrawing process of steel cord filament, Int. J. Refract. Met. Hard Mater. 26 (2008) 589–600.
[14] C Barbatti, F Sket, J García, A Pyzalla, Influence of Binder Metal and Surface Treatment on the Corrosion Resistance of (W,Ti)C-Based Hardmetals, Surface Coating Technol. 201 (2006) 3314–3327.
[15] W J Tomlinson, C R Linzell, Anodic polarization and corrosion of cemented carbides with cobalt and nickel binders, J. Mater. Sci. 23 (1988) 914–918.
[16] A M M Human, H E Exner, The relationship between electrochemical behaviour and in-service corrosion of WC based cemented carbides, Int. J. Refract. Met. Hard Mater. 15 (1997) 65–71.
[17] S Hochstrasser, Y Mueller, C Latkoczy, S Virtanen, P Schmutz, Analytical characterization of the corrosion mechanisms of WC-Co by electrochemical methods and inductively coupled plasma mass spectroscopy, Corros. Sci. 49 (2007) 2002–2020.
[18] D S Konadu, J Van der Merwe, J H Potgieter, S Potgieter-Vermaak, C N Machio, The corrosion behaviour of WC-VC-co hardmetals in acidic media, Corros. Sci. 52 (2010) 3118–3125.
[19] S Sutthiruangwong, G Mori, Corrosion properties of Co-based cemented carbides in acid solutions, Int. J. Refract. Met. Hard Mater. 21 (2003) 135–145.
[20] A J Gant, M G Gee, A T May, The evaluation of tribo-corrosion synergy for WC-Co hardmetals in low stress abrasion, Wear 256 (2004) 500–516.
[21] A J Gant, M G Gee, D D Gohil, H G Jones, L P Orkney, Use of FIB/SEM to assess the tribo-corrosion of WC/co hardmetals in model single point abrasion experiments, Tribol. Int. 68 (2013) 56–66.
[22] B Roebuck, E A Almond, Deformation and fracture process and the physical metallurgy of WC-Co hardmetals, Int. Mater. Rev. 33 (1988) 90–110.
[23] J M Tarragó, D Coureaux, Y Torres, F Wu, I Al-Dawery, L Llanes, Implementation of cemented carbides, Int. J. Refract. Met. Hard Mater. 55 (2016) 80–86.

[24] J M Brun, W B Thadis, Comparison of line intercepts and random point frames for sampling desert shrub vegetation, J. Range Manag. 16 (1963) 21–25.
[25] R H Canfield, Measurement of grazing use by the line intercept method, J. For. 42 (1944) 192–214.
[26] B R Lawn, Indentation of ceramics with spheres: a century after Hertz, J. Am. Ceram. Soc. 81 (1998) 1977.
[27] E Tarrés, G Ramírez, Y Gaillard, E Jiménez-Piqué, L Llanes, Contact fatigue behavior of PVD-coated hardmetals, Int. J. Refract. Met. Hard Mater. 27 (2009) 323–331.
[28] G Ramírez, A Mestra, B Casas, I Valls, R Martínez, R Bueno, A Gómez, A Mateo, L Llanes, Influence of substrate microstructure on the contact fatigue strength of coated col-worked tool steels, Surf. Coat. Technol. 206 (2012) 3069.
[29] H E Exner, The influence of sample preparation on Palmqvist's method for toughness testing of cemented carbides, Trans. AIME 245 (1969) 677.
[30] D K Shetty, I G Wright, P N Mincer, A H Clauer, Indentation fracture of WC-Co cermets, J. Mater. Sci. 20 (1985) 1873–1882.
[31] J A M Ferreira, M A Pina Amaral, F V Antunes, J D M Costa, A study on the mechanical behaviour of WC/Co hardmetals, Int. J. Refract. Met. Hard Mater. 27 (2009) 1–8.
[32] T A Fabijanic, D Coric, M S Musa, M Sakoman, Vickers indentation fracture toughness of near-nano and nanostructured WC-Co cemented carbides, Metals. 7 (2017) 1–17.
[33] B Johannesson, R Warren, Subcritical crack growth and plastic deformation in the fracture of hard metals, Mater. Sci. Eng. A. 105 (106) (1988) 353–361.
[34] L S Sigl, H F Fischmeister, On the fracture toughness of cemented carbides, Acta Metall. 36 (1988) 887–889.
[35] D Chen, L Yao, Z Chen, H Wang, W Peng, Investigation on the static fatigue mechanisms and effect of specimen thickness on the static fatigue lifetime in WC-Co cemented carbides, J. Superhard Mater. 40 (2018) 118–126.
[36] P R Fry, G G Garret, Fatigue crack growth behaviour of tungsten carbide-cobalt hardmetals, J. Mater. Sci. 23 (1988) 2325–2338.
[37] B D Wright, P J Green, P M Braiden, Quantitative analysis of delayed fracture observed in stress rate tests on brittle materials, J. Mater. Sci. 17 (1982) 3227–3234.
[38] S Sutthiraungwong, G Mori, R Kösters, Passivity and pseudopassivity of cemented carbides, Int. J. Refract. Met. Hard Mater. 23 (2005) 129–136.
[39] A Góez, D Coureaux, A Ingebrand, B Reig, E Tarrés, A Mestra, A Mateo, E Jiménez-Piqué, L Llanes, Contact damage and residual strength in hardmetals, Int. J. Refract. Met. Hard Mat. 30 (2012) 121–127.
[40] A C Fischer-Cripps, B R Lawn, Stress analysis of contact deformation in quasi-plastic ceramics, J. Am. Ceram. Soc. 79 (1996) 2609–2618.
[41] Y-W Rhee, H-W Kim, Y Deng, B R Lawn, Brittle fracture versus quasi plasticity in ceramics: a simple predictive index, J. Am. Ceram. Soc. 87 (2001) 561–565.
[42] H Zhang, Z Z Fang, J D Belnap, Quasi-plastic deformation of WC-Co composites loaded with a spherical indenter, Metall. Mater. Trans. 38A (2007) 552–561.
[43] B R Lawn, A G Evans, D B Marshall, Elastic/plastic indentation damage in ceramic: the median/radial crack system, J. Am. Ceram. Soc. 63 (1980) 574–580.
[44] A Yonezu, M Niwa, J Ye, X Chen, Contact fracture mechanism of electroplated Ni-P coating upon stainless steel substrate, Mater. Sci. Eng. A 563 (2013) 184–192.
[45] S Stewart, R Ahmed, Contact fatigue failure modes in hot isostatically pressed WC-12%Co coatings, Surf. Coat. Technol. 172 (2003) 204–216.
[46] H Engqvist, U Beste, N Axén, The influence of pH on sliding wear of WC-based materials, Int. J. Refract. Met. Hard Mater. 18 (2000) 109.
[47] F J J J Kellner, H Hildebrand, S Virtanen, Effect of WC grain size on the corrosion behavior of WC-Co based hardmetals in alkaline solutions, Int. J. Refract. Met. Hard Mater. 27 (2009) 806–812.
[48] J J Roa, E Jiménez-Piqué, J M Tarragó, M Zivcec, C Broeckmann, L Llanes, Berkovich nanoindentation and deformation mechanisms in a hardmetal binder-like cobalt alloy, Mater. Sci. Eng. A 621 (2015) 128–132.
[49] V K Sarin, T Johannesson, On the deformation of WC-Co cemented carbides, Met. Sci. 9 (1975) 472–476.
[50] B Roebuck, E A Almond, The influence of composition, phase transformation and varying the relative F.C.C. and H.C.P. phase contents on the properties of dilute Co-W-C Alloys, Mater. Sci. Eng 66 (1984) 179–194.
[51] C H Vasel, A D Krawitz, E F Drake, E A Kenik, Binder deformation in WC-(Co,Ni) cemented carbide composites, Metall. Mater. Trans. A 16A (1985) 2309–2317.
[52] G Erling, S Kursawe, S Luyck, H G Sockel, Stable and unstable fracture surface features in WC-Co, J. Mater. Sci. Lett. 19 (2000) 437–438.
[53] J M Tarragó, J J Roa, E Jiménez-Piqué, E Keown, J Fair, L Llanes, Mechanical deformation of WC-Co composite micropillars under uniaxial compression, Int. J. Ref. Met. Hard Mater. 54 (2016) 70–74.
[54] D A Sandoval, A Rinaldi, J M Tarragó, J J Roa, J Fair, L Llanes, Scale effect in mechanical characterization of WC-Co composites, Int. J. Ref. Met. Hard Mat. 72 (2018) 157–162.
[55] H F Fischmeister, S Schmauder, L S Sigl, Finite element modelling of crack propagation in WC-Co hard metals, Mater. Sci. Eng. A 105/106 (1988) 305–311.